Iterative Overlap TD-QRM-ML Block Signal Detection for Single-Carrier Transmission without CP Insertion

Hideyuki MOROGA† Tetsuya YAMAMOTO† and Fumiyuki ADACHI‡
Dept. of Electrical and Communication Engineering, Graduate School of Engineering, Tohoku University
6-6-05 Aza-Aoba, Aramaki, Aoba-ku, Sendai, 980-8579 Japan
†{moroga, yamamoto}@mobile.ecei.tohoku.ac.jp, ‡adachi@ecei.tohoku.ac.jp

***Abstract*—A time-domain maximum likelihood block signal detection employing QR decomposition and M-algorithm (TD-QRM-MLBD) is a computationally efficient near ML detection scheme and can significantly improve the bit error rate (BER) performance of the single-carrier (SC) transmissions in a frequency-selective fading channel, compared to the conventional minimum mean square error based frequency-domain equalization (MMSE-FDE). In TD-QRM-MLBD, the cyclic prefix (CP) is inserted in order to avoid inter-block interference (IBI). However, the CP insertion reduces the transmission efficiency. In this paper, we propose an iterative overlap TD-QRM-MLBD which requires no CP insertion. We evaluate the throughput performance of iterative overlap TD-QRM-MLBD by computer simulation to compare it with the conventional TD-QRM-MLBD with CP insertion.**

Keywords-component; Single-carrier, QRM-MLBD, time-domain signal detection, no cyclix prefix

I. INTRODUCTION

The wireless channel is composed of many propagation paths with different time delays, the channel becomes severely frequency-selective for broadband signal transmissions. In a severe frequency-selective fading channel, the bit error rate (BER) performance significantly degrades due to inter-symbol interference (ISI) when single-carrier (SC) transmission without equalization is used [1, 2].

The conventional minimum mean square error based frequency-domain equalization (MMSE-FDE) improves the SC transmission performance [3, 4], but it exhibits still a big performance gap from matched filter (MF) bound [5].

A frequency-domain block signal maximum likelihood detection (MLD) employing QR decomposition and M-algorithm (FD-QRM-MLBD) [6, 7] can significantly improve the BER performance of SC block transmissions compared to the MMSE-FDE. In FD-QRM-MLBD, the discrete Fourier transform (DFT) of the received signal is required. FD-QRM-MLBD is equivalent to time-domain QRM-MLBD (TD-QRM-MLBD) [8]. Since TD-QRM-MLBD does not require DFT of the received signal, it has an advantage over FD-QRM-MLBD in terms of the computational complexity.

In the conventional SC block transmission using MMSE-FDE, the insertion of cyclic prefix (CP) is used to avoid the inter-block interference (IBI) and make the received signal block to be a circular convolution of the transmitted block and channel impulse response. However, CP insertion reduces transmission efficiency. Therefore, an overlap MMSE-FDE [9, 10] which requires no CP insertion was proposed. However, it exhibits still a big performance gap from MF bound.

Without CP insertion, the performance of TD-QRM-MLBD degrades due to the residual IBI. The IBI is stronger on symbols near the end of block. Based on the above observation, we proposed an overlap TD-QRM-MLBD which suppresses the IBI in [8]. QRM-MLBD is applied to the received signal over the observation window. Then, only the reliable symbols are picked up to suppress the residual IBI. To detect a continuously transmitted symbol stream, the present observation window overlaps with previous and next observation windows. Therefore, the transmission efficiency is higher than that of the conventional TD-QRM-MLBD with CP insertion. However, the IBI suppression is not sufficient and the achievable performance improvement is limited by the residual IBI.

In this paper, we propose an iterative overlap TD-QRM-MLBD in order to effectively suppress the residual IBI. In iterative overlap TD-QRM-MLBD, the symbol order in the transmit symbol vector is reversed to suppress the IBI. A stopping criterion is introduced to reduce the computational complexity required for the path metric calculation. In this paper, we will investigate by computer simulation the throughput performance achievable by our proposed iterative overlap TD-QRM-MLBD to compare with the conventional TD-QRM-MLBD with CP insertion. We will also discuss the computational complexity of the proposed iterative overlap TD-QRM-MLBD.

The remainder of this paper is organized as follows. Sect. II presents the proposed iterative overlap TD-QRM-MLBD. In Sect. III, the throughput performance is evaluated by computer simulation to compare it with the conventional TD-QRM-MLBD with CP insertion. Computational complexity of the iterative overlap TD-QRM-MLBD is also discussed. Section IV concludes this paper.

978-1-4673-1881-5/12/$31.00 ©2012 IEEE

II. ITERATIVE OVERLAP TD-QRM-MLBD

A. Transmission System

Figure 1 shows the system model of SC transmission using the proposed iterative overlap TD-QRM-MLBD. Figure 2 shows block signal processing of iterative overlap TD-QRM-MLBD. Throughout the paper, the equivalent low-pass representation of discrete-time t normalized by the transmission symbol length T_s is used.

At the receiver, the received signal is divided into a sequence of blocks of X symbols to be picked up (called X-symbol block). The received signal $\mathbf{y}=[y(0),...,y(t),...,y(N_c+L-2)]^T$ of N_c+L-1 symbols (called the observation window) is stored to detect a block of N_c symbols including X-symbol block at the beginning, where L is the number of propagation paths. In the i-th iteration stage, the replica of IBI from the previous block is generated by using the i-th stage decision of previous block. The replica of IBI from the next block is generated by the $(i-1)$-th stage decision of next block. The IBIs are removed by subtracting its replicas from the received signal sequence over the observation window before applying QRM-MLBD. After QRM-MLBD, the first X-symbol block is picked up. To detect the next X-symbol block, the observation window is shifted by X-symbol block as shown in Fig. 2. By repeating this process I times (I=0 represents the initial detection), the residual IBI is suppressed.

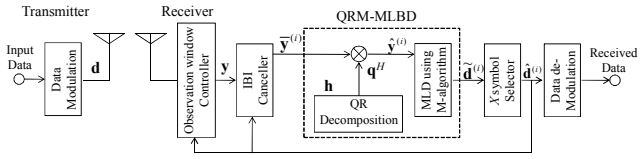

Figure 1. SC transmission using iterative overlap TD-QRM-MLBD.

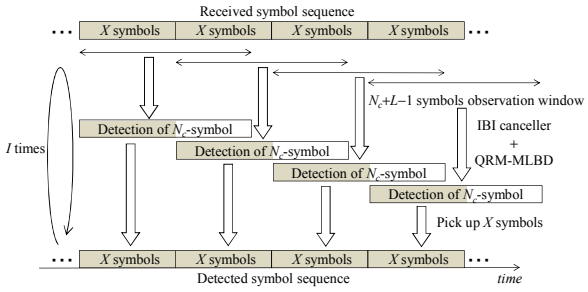

Figure 2. Iterative Overlap QRM-MLBD.

B. Received Signal Representation

The SC signal is transmitted over a frequency-selective fading channel composed of L propagation paths with different time delays. The channel impulse response $h(\tau)$ can be expressed as

$$h(\tau)=\sum_{l=0}^{L-1} h_l \delta(\tau-\tau_l), \tag{1}$$

where h_l and τ_l are respectively the complex-valued path gain with $E[\sum_{l=0}^{L-1}|h_l|^2]=1$ and the time delay of the l-th path. The l-th path time delay is assumed to be l symbols (i.e., $\tau_l=l$) and the path gains remain constant over at least an interval of the observation window. The received signal sequence $\mathbf{y}=[y(0),...,y(t),...,y(N_c+L-2)]^T$ of N_c+L-1 symbols over the observation window can be expressed using the matrix form as

$$\mathbf{y}=\sqrt{\frac{2E_s}{T_s}}\mathbf{h}\mathbf{d}+\sqrt{\frac{2E_s}{T_s}}\mathbf{h}_{-1}\mathbf{d}_{-1}+\sqrt{\frac{2E_s}{T_s}}\mathbf{h}_{+1}\mathbf{d}_{+1}+\mathbf{n}, \tag{2}$$

where $\mathbf{d}=[d(0),...,d(t),...,d(N_c-1)]^T$ represents the desired transmit symbol sequence. $\mathbf{d}_{-1}=[d_{-1}(0),...,d_{-1}(t),...,d_{-1}(N_c-1)]^T$ and $\mathbf{d}_{+1}=[d_{+1}(0),...,d_{+1}(t),...,d_{+1}(N_c-1)]^T$ represent the transmit symbol sequences in the previous block and in the next block, respectively. The first term of Eq. (2) represents the desired signal component. The second and the third terms represent the IBI components from the previous block and from the next block, respectively. $\mathbf{n}=[n(0),...,n(t),...,n(N_c+L-1)]^T$ is the noise vector. The t-th element, $n(t)$, of $\mathbf{n}$ is the zero-mean complex Gaussian variable having the variance $2N_0/T_s$ with N_0 being the one-sided power spectrum density of the additive white Gaussian noise (AWGN). E_s is the transmit symbol energy. $\mathbf{h}$, $\mathbf{h}_{-1}$, and $\mathbf{h}_{+1}$ are respectively an $(N_c+L-1)\times N_c$ channel impulse response matrixes given as

$$\begin{cases}\mathbf{h}=\begin{bmatrix} h_0 & & \mathbf{0} \\ \vdots & \ddots & \\ h_{L-1} & & \ddots \\ & \ddots & h_0 \\ & & \ddots \ \vdots \\ \mathbf{0} & & h_{L-1}\end{bmatrix}, \\ \mathbf{h}_{-1}=\begin{bmatrix} h_{L-1} & \cdots & h_1 \\ & \ddots & \vdots \\ & & h_{L-1} \\ & & \\ \mathbf{0} & & \end{bmatrix}, \mathbf{h}_{+1}=\begin{bmatrix} & & \mathbf{0} \\ & & \\ h_0 & & \\ \vdots & \ddots & \\ h_{L-2} & \cdots & h_0\end{bmatrix}.\end{cases} \tag{3}$$

C. Iterative Overlap TD-QRM-MLBD

In the i-th iteration stage, the IBI replica from the previous block is generated by using the decision of $\hat{\mathbf{d}}_{-1}^{(i)}=[\hat{d}_{-1}^{(i)}(0),...,\hat{d}_{-1}^{(i)}(t),...,\hat{d}_{-1}^{(i)}(N_c-1)]^T$ of the previous block. When $i\geq 1$, the IBI replica from the next block is generated by using the decision of $\hat{\mathbf{d}}_{+1}^{(i-1)}=[\hat{d}_{+1}^{(i-1)}(0),...,\hat{d}_{+1}^{(i-1)}(t),...,\hat{d}_{+1}^{(i-1)}(N_c-1)]^T$ of the next block. The IBI cancellation is performed by subtracting the IBI replicas from the received signal as

$$\begin{aligned}\overline{\mathbf{y}}^{(i)}&=\mathbf{y}-\sqrt{\frac{2E_s}{T_s}}\mathbf{h}_{-1}\hat{\mathbf{d}}_{-1}^{(i)}-\sqrt{\frac{2E_s}{T_s}}\mathbf{h}_{-1}\hat{\mathbf{d}}_{+1}^{(i-1)} \\ &=\sqrt{\frac{2E_s}{T_s}}\mathbf{h}\mathbf{d}+\sqrt{\frac{2E_s}{T_s}}\mathbf{h}_{-1}\left(\mathbf{d}_{-1}-\hat{\mathbf{d}}_{-1}^{(i)}\right) \\ &\quad+\sqrt{\frac{2E_s}{T_s}}\mathbf{h}_{+1}\left(\mathbf{d}_{+1}-\hat{\mathbf{d}}_{+1}^{(i-1)}\right)+\mathbf{n}\end{aligned}, \tag{4}$$

Identify applicable sponsor/s here. *(sponsors)*

where the second and the third terms of Eq. (4) are the residual IBIs from the previous and the next blocks, respectively.

In iterative overlap TD-QRM-MLBD, the symbol order in the desired transmit symbol vector $\mathbf{d}$ is reversed as $\mathbf{d}'=[d(N_c-1),...,d(t),...,d(0)]^T$. By doing so, the channel matrix $\mathbf{h}'$ is given as

$$\mathbf{h}'=\begin{bmatrix} \mathbf{0} & & & h_{L-1} \\ & \ddots & \iddots & \vdots \\ & \iddots & & h_0 \\ h_{L-1} & \ddots & & \\ \vdots & \iddots & & \\ h_0 & & & \mathbf{0} \end{bmatrix}. \tag{5}$$

QR decomposition is applied to $\mathbf{h}'$ as

$$\mathbf{h}'=\mathbf{qr}, \tag{6}$$

where $\mathbf{q}$ is an $(N_c+L-1)\times N_c$ unitary matrix satisfying $\mathbf{q}^H\mathbf{q}=\mathbf{I}$ ($\mathbf{I}$ is the identity matrix) and $\mathbf{r}$ is an $N_c\times N_c$ upper triangular matrix. $(.)^H$ denotes the Hermitian transpose operation. $\mathbf{q}$ and $\mathbf{r}$ obtained by QR decomposition of $\mathbf{h}'$ are represented as

$$\begin{cases} \mathbf{q}=\begin{bmatrix} \mathbf{0} & & & & q_{N_c-1,0} \\ & & & \iddots & \vdots \\ & & \iddots & & \vdots \\ & \iddots & & & \vdots \\ q_{0,N_c-1} & & & & \vdots \\ \vdots & & & & \vdots \\ q_{0,N_c+L-2} & \cdots & \cdots & \cdots & q_{N_c-1,N_c+L-2} \end{bmatrix} \\ \mathbf{r}=\begin{bmatrix} r_{0,0} & \cdots & r_{L-1,0} & & \mathbf{0} \\ & \ddots & & \ddots & \\ & & \ddots & & r_{N_c-L,N_c-1} \\ & & & \ddots & \vdots \\ \mathbf{0} & & & & r_{N_c-1,N_c-1} \end{bmatrix} \end{cases}. \tag{7}$$

By left multiplying $\mathbf{q}^H$ to $\bar{\mathbf{y}}^{(i)}$, we obtain the transformed vector given by

$$\begin{aligned} \hat{\mathbf{y}}^{(i)} &= \mathbf{q}^H\bar{\mathbf{y}}^{(i)} \\ &= \sqrt{\frac{2E_s}{T_s}}\mathbf{rd}'+\sqrt{\frac{2E_s}{T_s}}\hat{\mathbf{h}}_{-1}\left(\mathbf{d}_{-1}-\hat{\mathbf{d}}_{-1}^{(i)}\right), \\ &\quad +\sqrt{\frac{2E_s}{T_s}}\hat{\mathbf{h}}_{+1}\left(\mathbf{d}_{+1}-\hat{\mathbf{d}}_{+1}^{(i-1)}\right)+\hat{\mathbf{n}} \end{aligned} \tag{8}$$

where $\hat{\mathbf{h}}_{-1}=\mathbf{q}^H\mathbf{h}_{-1}$, $\hat{\mathbf{h}}_{+1}=\mathbf{q}^H\mathbf{h}_{+1}$, and $\hat{\mathbf{n}}=\mathbf{q}^H\mathbf{n}$. From Eq. (8), ML solution can be expressed as

$$\tilde{\mathbf{d}}_{ML}=\arg\min_{\bar{\mathbf{d}}\in Z^{N_d}}\left\|\hat{\mathbf{y}}-\sqrt{\frac{2E_s}{T_s}}\mathbf{r}\bar{\mathbf{d}}\right\|^2, \tag{9}$$

where Z is the modulation level (e.g., Z=16 for 16QAM). $\bar{\mathbf{d}}$ is the candidate symbol vector. Thanks to the upper triangular structure of $\mathbf{r}$, MLD can be done using an N_c-stages M-algorithm [11] to reduce the computational complexity. The M-algorithm keeps only M most reliable paths as surviving paths at each stage. The most likely transmitted symbol sequence is found by tracing back the surviving path having the smallest accumulated path metric at the last stage. The branch metric $e_n'^{(i)}$ and the accumulated path metric $e_n^{(i)}$ at the n-th stage (n=0, 1,…, N_c–1) are defined as

$$\begin{cases} e_n'^{(i)}=\left|\hat{y}^{(i)}(N_c-1-n')-\sqrt{\frac{2E_s}{T_s}}\sum_{t=0}^{n'}r_{N_c-1-n',N_c-1-t}\bar{d}(t)\right|^2, \\ e_n^{(i)}=\sum_{n'=0}^{n}e_n'^{(i)} \end{cases} \tag{10}$$

where $\bar{d}(t)$ is the candidate symbol for $d(t)$. It is understood from Eq. (7) that the nth ($n\le N_c-L$) row of $\mathbf{r}$ has non-zero element in the n~(n+L–1)-th columns only. This is because the channel impulse response has the length of L symbols. Hence, the branch metric $e_n'^{(i)}$ in Eq. (10) can be rewritten as

$$e_n'^{(i)}=\left|\hat{y}^{(i)}(N_c-1-n')-\sqrt{\frac{2E_s}{T_s}}\sum_{t=n'-L+1}^{n'}r_{N_c-1-n',N_c-1-t}\bar{d}(t)\right|^2. \tag{11}$$

The computation of branch metric after L stage doesn't affect the detection of the t-th symbol $d(t)$. Therefore, the M-algorithm can be stopped at the X+L–1th (X+L–1$\le N_c$) stage to pick up X-symbol block. The most probable transmitted symbol sequence is found by tracing back the surviving path having the smallest accumulated path metric at the X+L–1 stage.

When CP is not inserted, the IBI from both the previous and the next blocks is present. In the initial iteration stage (i=0), the IBI from the previous block can be suppressed by using the decision of previous block as Eq. (4). However, the IBI from the next block cannot be removed. Here, we consider the distribution of IBI from the next block after multiplying $\mathbf{q}^H$. The IBI from the next block (third term of Eq. (8)) can be given as

$$\begin{cases} \sqrt{\frac{2E_s}{T_s}}\hat{\mathbf{h}}_{+1}\mathbf{d}_{+1}=\sqrt{\frac{2E_s}{T_s}}\mathbf{q}^H\mathbf{h}_{+1}\mathbf{d}_{+1} \\ =\sqrt{\frac{2E_s}{T_s}}\begin{bmatrix} \hat{h}_{+10,0} & \cdots & \hat{h}_{+10,L-2} & \\ \vdots & & \vdots & \\ \vdots & & \vdots & \mathbf{0} \\ \vdots & & \vdots & \\ \hat{h}_{+1N_c-1,0} & \cdots & \hat{h}_{+1N_c-1,L-2} & \end{bmatrix}\begin{bmatrix} d_{+1}(N_c-1) \\ \vdots \\ \vdots \\ d_{+1}(0) \end{bmatrix} \end{cases}. \tag{12}$$

It can be seen from Eq. (7) that the absolute value of each element of $\mathbf{q}^H$ is larger in upper row vector since $\mathbf{q}^H$ is unitary matrix. Therefore, the absolute value of each element of $\hat{\mathbf{h}}_{+1}$ in Eq. (12) are larger in upper row vector. Figure 3 plots the average IBI power from the next block, normalized by the

transmit power contained in $\hat{y}^{(0)}(t)$ for the initial iteration stage (i=0) for N_c=64. The IBI power associate with the t-th element of $\hat{y}^{(0)}(t)$ can be given by $E[\sum_{j=0}^{N_c-1}|\hat{h}_{+1t,j}|^2]$. It can be seen from Fig. 3 that the IBI power from the next block is less significant at the symbol closer to the end of the block. On the other hand, the IBI power from the next block is more significant at the symbol closer to the beginning of the block. Hence, the probability of removing the correct path is lower at early stages of the M-algorithm. On the other hand, the probability of removing the correct path is higher at last stages in the M-algorithm due to the stronger IBI. Therefore, only the reliable first X-symbol block $\hat{\mathbf{d}}^{(0)}=[\tilde{d}^{(0)}(0),...,\tilde{d}^{(0)}(t),...,\tilde{d}^{(0)}(X-1)]^T$ is picked up from the block.

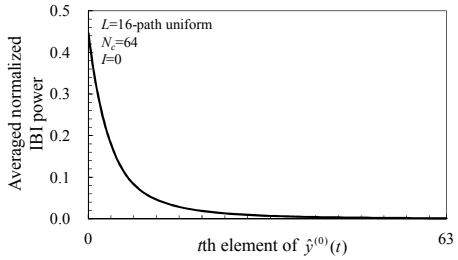

Figure 3. Averaged normalized IBI power associate with the t-th element of $\hat{y}^{(0)}(t)$.

III. Computer Simulation

We consider uncoded 16QAM transmission, packet size N_p=192, and GI length N_g=0. The channel is assumed to be a frequency-selective block Rayleigh fading channel having L=16-path uniform power delay profile and the normalized time delay $\tau_l=l$ symbols. We assume that there is no fading variation in one packet and ideal channel estimation is assumed.

A. Throughput Performance

Figure 4 plots the throughput performance as a function of average received E_s/N_0 with X (the number of symbols to be picked up) as a parameter for N_c=64 and M=4 (the number of surviving paths). The results for six cases of X are plotted, i.e., X=4, 8, 16, 32, 48, and 64. The use of M=4 is sufficient and therefore, only the throughput performance curve with M=4 is plotted. Throughput is defined as $\log_2 Z\times(1-\text{PER})/(1+N_g/N_c)$, where PER denotes the packet error rate. The throughput performance of the conventional TD-QRM-MLBD with CP insertion is also plotted for comparison. The training sequence (TS) aided QRM-MLBD with GI length of 16 symbols [12] is used similar to the conventional QRM-MLBD with CP insertion.

It can be seen from Fig. 4 that iterative overlap TD-QRM-MLBD improves the throughput performance by reducing X. This is because at early stages of M-algorithm, the IBI from the next block is less significant.

With no iteration (I=0), X=8 is required to achieve sufficiently improved throughput performance. However, when I=1 and 2, much larger X (e.g, X=32 and 48, respectively) can be used to achieve sufficiently improved throughput performance. Since iterative overlap TD-QRM-MLBD does not require the CP insertion, the throughput is higher than that of the conventional TD-QRM-MLBD with CP insertion.

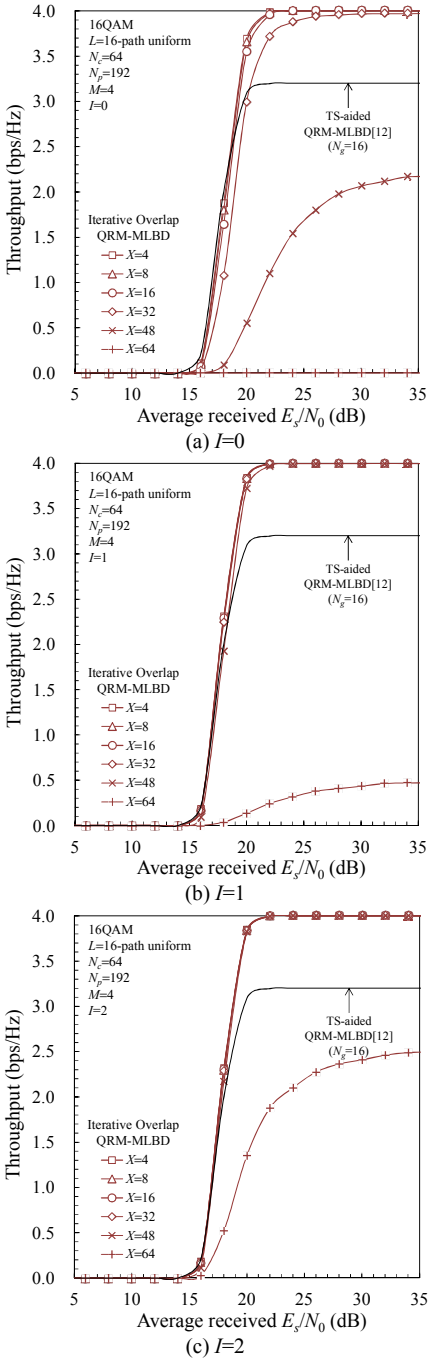

Figure 4. Throughput performance.

B. Computational Complexity

In this paper, the computational complexity is defined as the number of real multiplications per symbol. The complexities of iterative overlap TD-QRM-MLBD and the conventional TD-QRM-MLBD with CP insertion (TS-aided QRM-MLBD [12]) are shown in Table I. The number S of stages in the M-algorithm is given as

$$S = \begin{cases} X + L - 1 & (X < N_c - L + 1) \\ N_c & (X \geq N_c - L + 1) \end{cases}. \quad (13)$$

The complexity for the required X is shown in Figure 5 as a function of the number I of iterations for M=4. The complexity of the TD-QRM-MLBD with CP insertion is also plotted. The required X is 8 for I=0 and that can be increased to 32 for I=1. Therefore, the required complexity can be reduced even if iterative processing is involved.

Next we discuss the relationship between the number of N_c and the computational complexity. The best combination of I and X which achieves the peak throughput with lowest complexity is shown in Figure 6. When N_c is smaller, the complexity of the QR decomposition reduces since the channel matrix size is small. However, the complexity of the path metric is large. This is because larger I and smaller X are needed since the IBI is significant. It is understood from Fig. 6 that the complexity is lowest when N_c=34 and is about 0.95 times that of the conventional TD-QRM-MLBD (N_c=64) with CP insertion.

TABLE I. NUMBER OF REAL MULTIPLICATIONS PER SYMBOL

	Iterative Overlap TD-QRM-MLBD	TS-aided QRM-MLBD[12]
QR decomposition	$\{L(4L^2-3L+1)+(2L-1)(N_c-L)(N_c+3L-1)\}/N_p$	$\{L(4L^2-3L+1)+(2L-1)(N_c-L)(N_c+3L-1)\}/N_p$
IBI cancellation	$\sqrt{Z}\ L/N_p$	
Computation of $\hat{\mathbf{y}}$,	$2S(2N_c+2L-S-1)/X$ $+2(2S+L)(L-1)I/X$	$2N_c(N_c+2L-1)/N_c$
Path metric calc.	$\sqrt{Z}\ L(2S-L+1)/2N_p$ $+\{Z+MZ(S-1)\}2(I+1)/X$	$\sqrt{Z}\ L(2N_c-L+1)/2N_p$ $+\{Z+MZ(N_c-1)\}2/N_c$

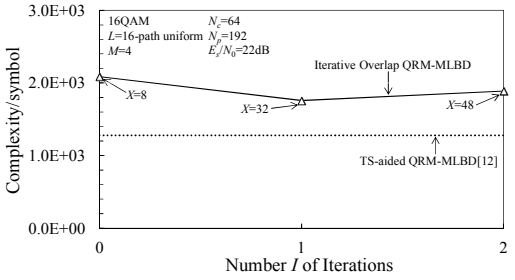

Figure 5. Impact of I and X on complexity.

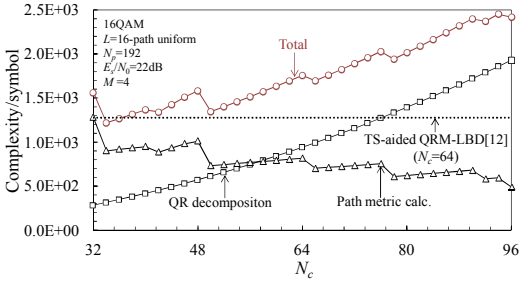

Figure 6. Impact of N_c on complexity

IV. CONCLUSIONS

In this paper, we proposed an iterative overlap TD-QRM-MLBD which requires no CP insertion. Exploiting the fact that the IBI exists near the end of the symbols in the block, only the reliable symbols are picked up after QRM-MLBD. To detect a continuously transmitted symbol stream, the present observation window overlaps with previous and next observation windows. To improve the IBI suppression, iterative processing and IBI cancellation are introduced. In iterative overlap TD-QRM-MLBD, M-algorithm can be truncated. Therefore the computational complexity required for the path metric calculation can be reduced. The complexity is about 0.95 times that of the conventional TD-QRM-MLBD with CP insertion. We showed that the iterative overlap TD-QRM-MLBD achieves about 1.25 times higher throughput than the conventional TD-QRM-MLBD with CP insertion (N_c=64, N_g=16).

REFERENCES

[1] W. C., Jakes Jr., Ed,. *Microwave mobile communications*, Wiley, New York, 1974.

[2] J. G. Proakis, and M Salehi, *Digital communications*, 5th ed., McGraw-Hill, 2008.

[3] D. Falconer, S. L. Ariyavisitakul, A. Benyamin-Seeyar, and B. Edison, "Frequency domain equalization for single-carrier broadband wireless systems," IEEE Commun. Mag., Vol. 40, No. 4, pp. 58-66. Apr. 2002.

[4] F. Adachi, T. Sao, and T. Itagaki, "Performance of multicode DS-CDMA using frequency domain equalization in a frequency selective fading channel," IEE Electronics Letters, Vol. 39, No.2, pp.239-241, Jan. 2003.

[5] F. Adachi and K. Takeda, "Bit error rate analysis of DS-CDMA with joint frequency-domain equalization and antenna diversity combining," IEICE Transactions on Communications, vol. E87-B, no. 10, pp. 2991–3002, 2004.

[6] K. Nagatomi, K. Higuchi, and H. Kawai, "Complexity reduced MLD based on QR decomposition in OFDM-MIMO multiplexing with frequency domain spreading and code multiplexing." Proc. IEEE Wireless Communications and Networking Conference (WCNC), Apr. 2009.

[7] T. Yamamoto, K. Takeda, and F. Adachi, "Single-carrier transmission using QRM-MLD with antenna diversity," Proc. The 12th International Symposium on Wireless Personal Multimedia Communications (WPMC 2009), Sept. 2009.

[8] H. Moroga, T. Yamamoto, and F. Adachi, "Overlap QRM-ML block signal detection for single-carrier transmission without CP insertion," Proc. IEEE 75th Vechular Technology Conference (VTC2012-Spring), May. 2012.

[9] I. Martoyo, T. Weiss, F. Capar, and F. K. Jondral, "Low complexity CDMA downlink receiver based on frequency domain equalization," Proc. IEEE 58th Vechular Technology Conference (VTC2003), Sept. 2003.

[10] T. Takeda, H. Tomeba, and F. Adachi, "Iterative overlap FDE for DS-CDMA without GI," Proc. IEEE 64th Vechular Technology Conference (VTC2006-Fall), Sept. 2006.

[11] J. B. Anderson and S. Mohan, "Sequential coding algorithms: A survey and cost analysis," IEEE Trans. on Commun., Vol. 32, pp. 169-176, Feb. 1984.

[12] T. Yamamoto, K. Takeda and F. Adachi, "Frequency-domain block signal detection with QRM-MLD for training sequence-aided single-carrier transmission," EURASIP Journal on Advances in Signal Processing, Vol. 2011.